pubs.acs.org/acschemicalbiology

Articles

Targeted Protein Degradation through E2 Recruitment

Nafsika Forte, Dustin Dovala, Matthew J. Hesse, Jeffrey M. McKenna, John A. Tallarico, Markus Schirle, and Daniel K. Nomura*

Cite This: https://doi.org/10.1021/acschembio.3c00040

Read Online

ACCESS | Metrics & More | Article Recommendations | Supporting Information

ABSTRACT: Targeted protein degradation (TPD) with proteolysis targeting chimeras (PROTACs), heterobifunctional compounds consisting of protein targeting ligands linked to recruiters of E3 ubiquitin ligases, has arisen as a powerful therapeutic modality to induce the proximity of target proteins with E3 ligases to ubiquitinate and degrade specific proteins in cells. Thus far, PROTACs have primarily exploited the recruitment of E3 ubiquitin ligases or their substrate adapter proteins but have not exploited the recruitment of more core components of the ubiquitin-proteasome system (UPS). In this study, we used covalent chemoproteomic approaches to discover a covalent recruiter against the E2 ubiquitin conjugating enzyme UBE2D—EN67—that targets an allosteric cysteine, C111, without affecting the enzymatic activity of the protein. We demonstrated that this UBE2D recruiter could be used in heterobifunctional degraders to degrade neo-substrate targets in a UBE2D-dependent manner, including BRD4 and the androgen receptor. Overall, our data highlight the potential for the recruitment of core components of the UPS machinery, such as E2 ubiquitin conjugating enzymes, for TPD, and underscore the utility of covalent chemoproteomic strategies for identifying novel recruiters for additional components of the UPS.

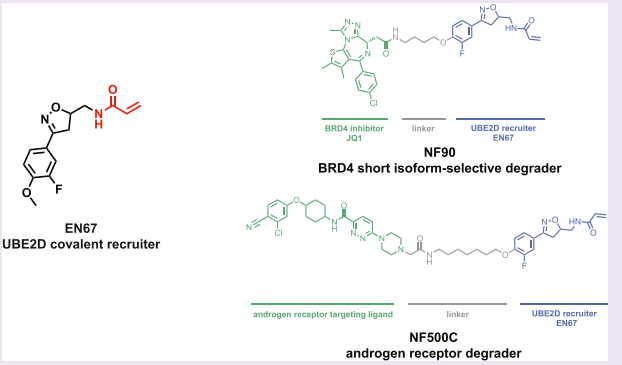

INTRODUCTION

Targeted protein degradation (TPD) using proteolysis targeting chimeras (PROTACs) or molecular glues has arisen as a powerful therapeutic modality for chemically inducing the proximity of E3 ubiquitin ligases with proteins that do not natively interact with each other or "neo-substrate" target proteins to ubiquitinate and degrade specific proteins through the proteasome.[1,2] Despite the widespread development of PROTACs for many target proteins, most PROTACs have utilized recruiters against only a select few E3 ligases or substrate receptors despite the existence of >600 protein factors within the ubiquitin-proteasome system (UPS).[3] Most PROTACs have employed recruiters against cereblon and VHL, with additional utilization of MDM2, cIAP, and DCAF15 recruiters.[3] Covalent chemoproteomic approaches have also revealed the ligandability of proteins within the UPS machinery and have led to the discovery of several additional recruiters against DCAF16, DCAF11, DCAF1, RNF114, RNF4, and FEM1B.[3−11] However, these recruiters thus far have all been against either E3 ligases or the substrate receptors of Cullin E3 ligase complexes and have not exploited more core and shared components of the UPS system, such as E2 ubiquitin-conjugating enzymes or commonly shared adapter proteins in Cullin E3 ligases (e.g., DDB1 or SKP1).

Recent discoveries of molecular glue degraders and their mechanisms reveal the conceptual possibility of exploiting these core UPS components in PROTACs. The CDK inhibitor CR8 was found to act as a molecular glue degrader that forms a ternary complex between the CUL4 adaptor protein DDB1 and the CDK12-cyclin K complex to induce the ubiquitination and degradation of cyclin K.[12] HQ461 was also found to promote ternary complex formation between CDK12 and DDB1 as well to induce the ubiquitination and degradation of cyclin K.[13] Our group also recently discovered the anticancer covalent ligand EN450, which recognizes the allosteric C111 on UBE2D conferring recognition for the transcription factor NFKB1—leading to its ubiquitination and proteasome-dependent degradation.[14] While these discoveries were all with molecular glue degraders and not PROTACs, they speak to the possibility that these core components of the Cullin complex (adapter proteins and E2s) can be recruited with small molecules to form ternary complexes with neo-substrate proteins to induce their ubiquitination and degradation. Recruitment of these core components of the UPS system, which are essential genes for many Cullin E3 ligase complexes and also for cell viability, may enable degradation of a broader or different scope of neo-substrates and potentially avoid resistance mechanisms to

Received: January 19, 2023
Accepted: March 9, 2023

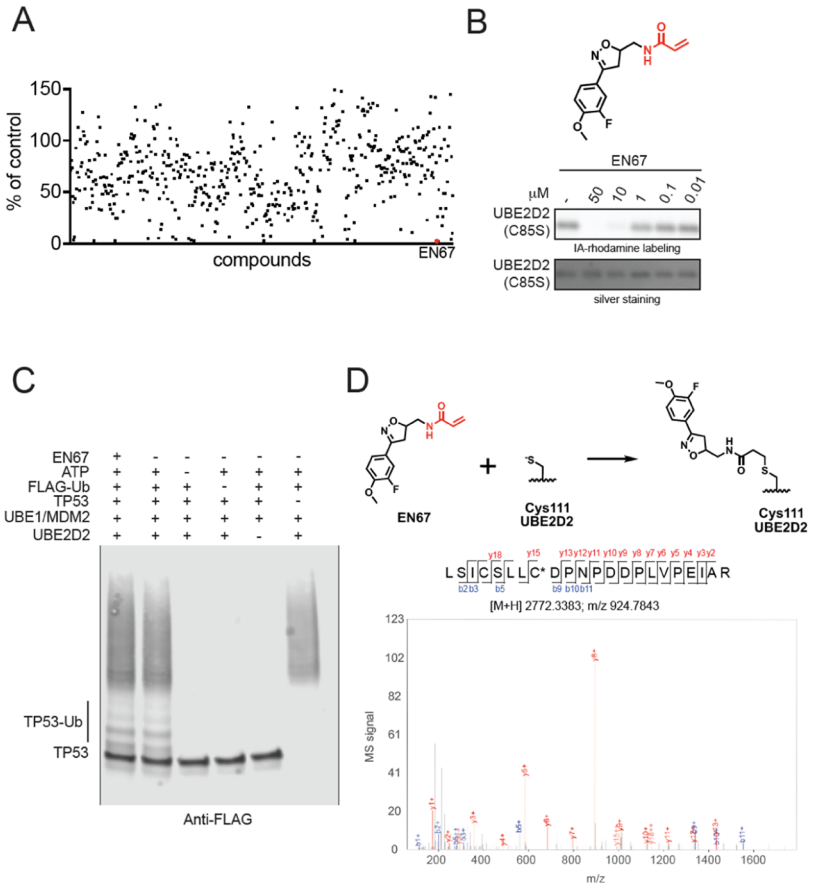

Figure 1. Discovering a covalent recruiter for E2 ubiquitin conjugating enzyme UBE2D. (A) Gel-based ABPP screen of cysteine-reactive covalent ligands against human pure UBE2D2 C85S protein showing EN67 as the top hit. (B) Structure of EN67 with the cysteine-reactive acrylamide warhead highlighted in red. Gel-based ABPP showing competition of EN67 against IA-rhodamine binding to UBE2D2 C85S pure protein and silver staining of protein showing equal protein loading. (C) TP53 ubiquitination activity by E1 UBE1, E2 UBE2D2, E3 MDM2, FLAG-ubiquitin, and ATP showing that EN67 does not inhibit TP53 ubiquitination activity. (D) Mapping of EN67 site of modification on human pure UBE2D2 C111 by LC-MS/MS. Experiments in (B), (C), and (D) are representative of $n = 3$ biological replicates/group.

PROTACs that exploit nonessential E3 ligase substrate receptors, such as cereblon.[15,16]

In this study, we sought to determine whether E2 ubiquitin conjugating enzymes can be recruited for heterobifunctional PROTAC applications. E2 ubiquitin conjugating enzymes accept ubiquitin from the E1 complex and catalyze its covalent attachment to other proteins.[17] Using covalent chemoproteomic approaches, we discovered a covalent recruiter that targets the allosteric C111 on the E2 UBE2D and showed that this recruiter can be used in PROTACs to degrade neo-substrate proteins in a UBE2D-dependent manner.

RESULTS AND DISCUSSION

Developing a Covalent Recruiter against the E2 Ubiquitin Conjugating Enzyme UBE2D. Among the E2 ubiquitin conjugating enzymes, we prioritized efforts to discover covalent recruiters against the UBE2D family, which consists of nearly identical isoforms UBE2D1, UBE2D2, UBE2D3, and UBE2D4 that all bear an active-site ubiquitin conjugating C85 as well as an allosteric cysteine C111 since we recently discovered a covalent molecular glue degrader EN450 that exploited this allosteric C111 without targeting the ubiquitin-conjugating C85.[14,17] This recent discovery pointed to the potential feasibility for recruitment of UBE2D for PROTACs. UBE2D1-4 are utilized as a ubiquitin-transfer enzyme for many different types of RING E3 ligases and Cullin E3 ligase complexes.[18,19] Given that we previously showed that EN450 covalently targeted C111 on UBE2D, albeit not very potently with midmicromolar affinity,[14] we initially developed NF142, a PROTAC linking EN450 to the BET family inhibitor JQ1 through a C4 alkyl linker (Figure S1A). NF142 dose-responsively competed against fluorophore-functionalized cysteine-reactive idoacetamide probe (IA-rhodamine) labeling of recombinant UBE2D2 C85S mutant protein at mid- to low-micromolar concentrations by gel-based activity-based protein profiling (ABPP) (Figure S1B).[10] When treated in HEK293T cells, NF142 modestly degraded only the short isoform of BRD4 by ~70% without degrading the long BRD4 isoform (Figure S1C,D).

Given that EN450 was discovered through a phenotypic screen for molecular glue degraders and not through a directed screen against UBE2D, we next screened a library of 569 cysteine-reactive acrylamide and chloroacetamide covalent ligands against recombinant human UBE2D2 C85S protein by gel-based ABPP competing the binding of covalent ligands against IA-rhodamine labeling (Figure 1A and Table S1). Through this screen, we identified EN67 as the top hit that dose-responsively bound to UBE2D2 (Figure 1B). Through reconstitution of TP53 ubiquitination activity by the E1 ubiquitin-activating enzyme, UBE2D2, MDM2, ubiquitin, and ATP, we confirmed that EN67 does not inhibit overall TP53

https://doi.org/10.1021/acschembio.3c00040
ACS Chem. Biol. XXXX, XXX, XXX−XXX

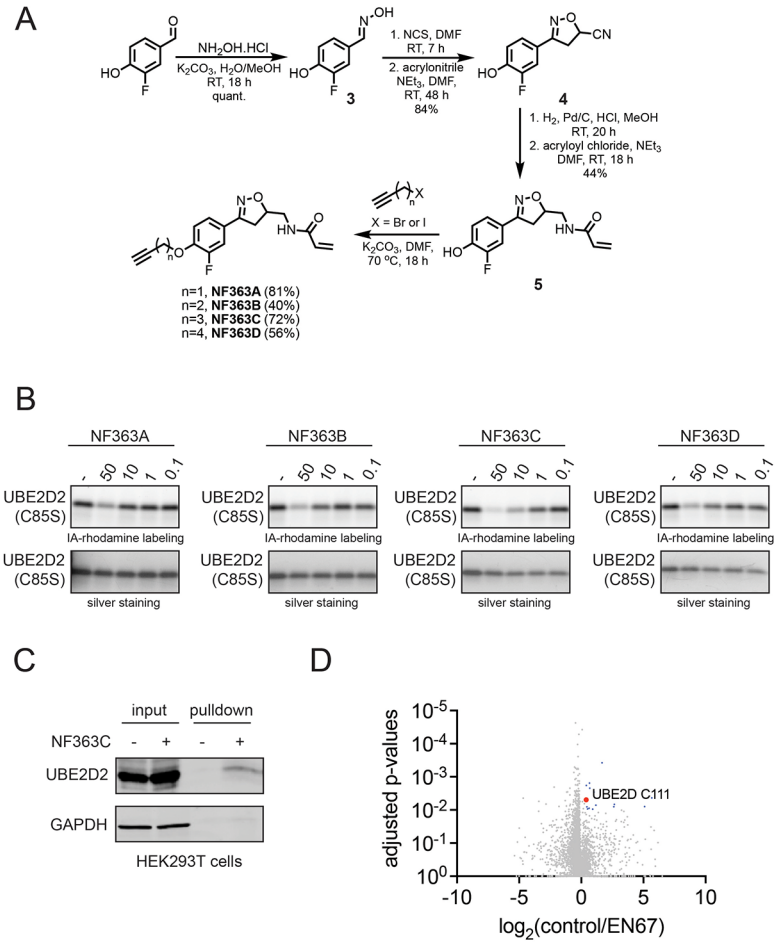

Figure 2. Validating target engagement and selectivity of EN67 in cells. (A) Synthetic route for making the alkyne-functionalized probe of EN67. (B) Gel-based ABPP of alkyne-functionalized EN67 probes against pure recombinant human UBE2D2 C85S protein and corresponding silver staining. (C) NF363C engagement and enrichment of UBE2D2 in HEK293T cells. Cells were treated with dimethyl sulfoxide (DMSO) or NF36C (50 μM) for 24 h. Probe-modified proteins were subsequently appended with an azide-functionalized biotin handle by CuAAC, and proteins were avidin-enriched and eluted for detection of UBE2D2 and an unrelated negative control protein GAPDH by Western blotting. Both input and pulldown of UBE2D2 and GAPDH are shown. (D) isoDTB-ABPP cysteine chemoproteomic profiling of EN67 in HEK293T cells. HEK293T cells were treated with DMSO vehicle or EN67 (50 μM) for 4 h. Lysates were labeled with IA-alkyne (200 μM) for 1 h, and isotopic desthiobiotin tags were appended by CuAAC and taken through the isoDTB-ABPP procedure. Shown are ratios of control/EN67-treated probe-modified peptide ratios and adjusted p-values from $n = 3$ biological replicates/group. Data are shown in Table S2. Data in panels (B) and (C) are representative of $n = 3$ biological replicates/group.

ubiquitination mediated by UBE2D2 and the whole ubiquitination machinery, suggesting the activity of UBE2D is not compromised by the EN67 covalent adduct (Figure 1C). We further mapped the site of modification of the EN67 covalent adduct on pure recombinant human wild-type UBE2D2 through liquid-chromatography-tandem mass spectrometry (LC-MS/MS) analysis of resulting tryptic digests and demonstrated that EN67 selectively targeted C111 without targeting the catalytic C85 (Figure 1D).

Assessing Target Engagement and Selectivity of UBE2D by EN67. We next sought to confirm target engagement and overall proteome-wide selectivity of EN67 for C111 of UBE2D in cells. We synthesized four alkyne-functionalized probes of EN67 with different spacer lengths (Figure 2A). NF363C exhibited the highest degree of binding to UBE2D2 (C85S) via gel-based ABPP (Figure 2B). Using this alkyne-functionalized probe, we showed engagement and enrichment of UBE2D2 but not unrelated proteins such as GAPDH from treatment of this probe in HEK293T cells, followed by appending on a biotin−azide enrichment handle by copper-catalyzed azide−alkyne cycloaddition (CuAAC) in resulting lysates, avidin-enrichment, and blotting for specific targets (Figure 2B,C). To assess the proteome-wide selectivity, cysteine reactivity, and degree of UBE2D2 engagement, we next performed isotopically labeled desthiobiotin tag-based ABPP (isoDTB-ABPP) competing in situ EN67 treatment in HEK293T cells against the alkyne-functionalized iodoacetamide (IA-alkyne) probe.[4,20,21] Among 3798 probe-modified peptides detected and quantified across all three biological replicates, there were only 11 targets that showed control vs EN67-treated probe-modified peptide ratios greater than 1.3 with an adjusted p-value of less than 0.01, among which C111 of UBE2D was the only protein involved in the UPS, showing a ratio of 1.3 (Figure 2D and Table S2). The specific C111 UBE2D ratio of 1.32 between control versus treated groups, also interpreted as the treated probe-modified peptide showing 76% area under the curve compared to control, indicated approximately 24% target engagement of UBE2D in cells. The other targets—GATA6, HK2, WDSUB1, SON, AK6, GTSE1, PYGO2, ACAA2, ASXL2, and ANP32A—were not related to the UPS and not expected to

https://doi.org/10.1021/acschembio.3c00040
ACS Chem. Biol. XXXX, XXX, XXX−XXX

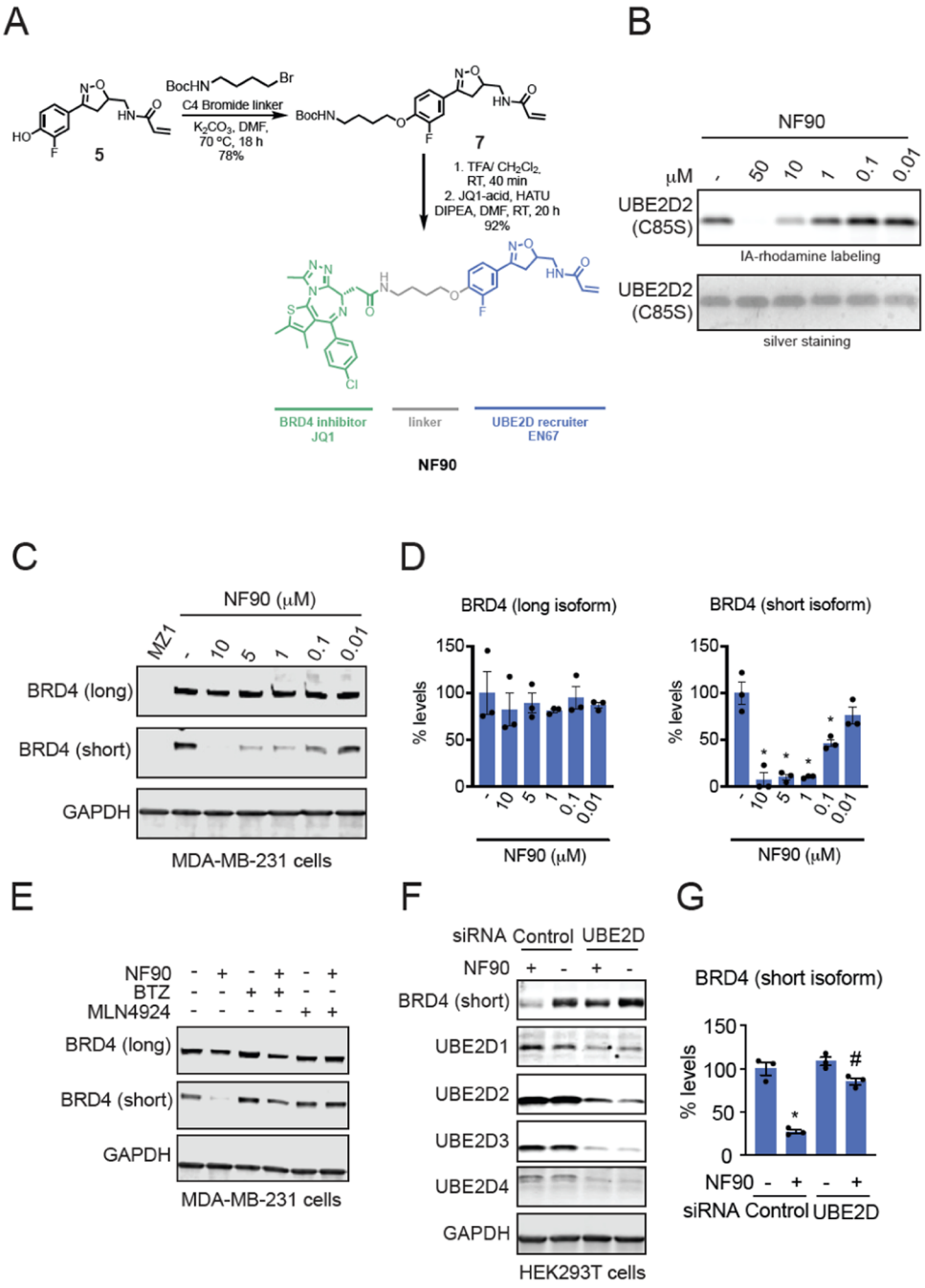

Figure 3. UBE2D-based BRD4 degrader. (A) Synthetic route and structure for NF90 linking UBE2D recruiter EN67 to BRD4 inhibitor JQ1. (B) Gel-based ABPP analysis of NF90 against IA-rhodamine labeling of pure human UBE2D2 C85S protein and corresponding silver staining. (C) NF90 effects on BRD4 levels in MDA-MB-231 breast cancer cells. MDA-MB-231 cells were treated with DMSO vehicle or NF90 for 24 h, and BRD4 and loading control GAPDH levels were assessed by Western blotting. (D) BRD4 levels from (C) quantified. (E) Attenuation of BRD4 degradation by a proteasome inhibitor bortezomib (BTZ) or a NEDDylation inhibitor (MLN4924). MDA-MB-231 cells were pre-treated with DMSO vehicle, BTZ (1 μM), or MLN4924 (1 μM) for 1 h prior to treatment of cells with DMSO vehicle or NF90 (10 μM) for 24 h. BRD4 and loading control GAPDH levels were assessed by Western blotting. (F) NF90 effects on BRD4 degradation upon UBE2D knockdown. HEK293T cells with siControl or siRNA knockdown of UBE2D1, UBE2D2, UBE2D3, and UBE2D4 treated with DMSO vehicle or NF90 (10 μM) for 24 h. BRD4 short isoform and UBE2D1-4 and loading control GAPDH were assessed by Western blotting. (G) BRD4 levels quantified from panel (F). Gels and blots shown in panels (B), (C), (E), and (F) are representative of $n = 3$ biological replicates/group. Bar graphs shown in panels (D) and (G) show average ± standard error of the mean (sem) with individual replicate values. Statistical significance compared to vehicle-treated control expressed as $^{*}p < 0.05$ and compared to NF90-treated siControl cells as $^{\#}p < 0.05$.

interfere with validating EN67 as a UBE2D recruiter in TPD applications. We note that the tryptic peptide sequence bearing C111 detected and quantified by isoDTB-ABPP is identical across UBE2D1, UBE2D2, UBE2D3, and UBE2D4, and thus, we cannot distinguish between them. Given the high degree of sequence identity between these UBE2D enzymes, we believe that EN67 likely targets all four isoforms of UBE2D. We deemed the relatively modest degree of engagement of UBE2D in cells to be acceptable given previous studies indicating that only fractional occupancy would likely be required to enable target

https://doi.org/10.1021/acschembio.3c00040
ACS Chem. Biol. XXXX, XXX, XXX−XXX

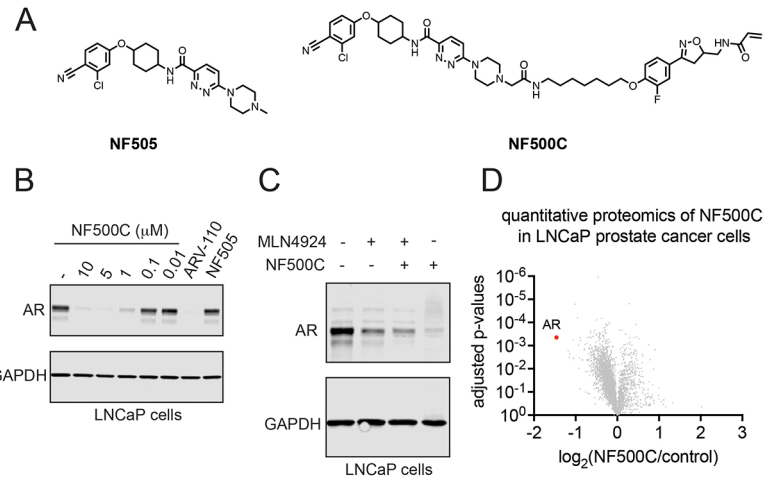

Figure 4. UBE2D-based AR degrader. (A) Structure of AR-targeting ligand control NF505 and UBE2D-based AR degrader NF500C linking the AR-targeting ligand to EN67. (B) AR degradation by NF500C. LNCaP prostate cancer cells were treated with DMSO vehicle or NF500C for 24 h and AR and loading control GAPDH levels were assessed by Western blotting. (C) AR degradation attenuated by NEDDylation inhibitor MLN4924. LNCaP cells were pre-treated with DMSO vehicle or NEDDylation inhibitor MLN4924 (1 μM) for 1 h prior to treating cells with DMSO vehicle or NF500C (10 μM) for 24 h. AR and loading control GAPDH levels were assessed by Western blotting. (D) TMT-based quantitative proteomic profiling of protein level changes conferred by NF500C treatment in LNCaP cells. LNCaP cells were treated with DMSO vehicle or NF500C (10 μM) for 24 h. Data are from n = 3 biological replicates/group. Gels and blots in panels (B) and (C) are representative of n = 3 biological replicates/group.

degradation with heterobifunctional compounds that demonstrate sub-stoichiometric activity.[5,8,9,22]

Testing EN67 as a UBE2D Recruiter for PROTAC Applications. Having shown that EN67 covalently targets C111 relatively selectively in cells, at least among the UPS, we next sought to demonstrate its utility in PROTACs to degrade neo-substrate proteins. We synthesized five PROTACs linking the EN67 UBE2D recruiter to the BET family inhibitor JQ1 with either a C2, C4, C5, C7 or PEG3 linker—NF129, NF90, NF369, NF370, and NF91, respectively (Figures 3A and S2A). These degraders still exhibited midmicromolar potency against UBE2D2 C85S by gel-based ABPP, showing displacement of cysteine-reactive probe labeling of pure protein (Figures 3B and S2B–D). We tested these degraders in HEK293T or MDA-MB-231 breast cancer cells. Only NF90, among the five degraders, demonstrated degradation of only the short, but not long, isoform of BRD4 in both HEK293T and MDA-MB-231 cells (Figure 3C,D, S2E–H, S3A,B). NF90 degraded BRD4 starting around 6 h of treatment with progressively increasing degradation through 24 h (Figure S3C). JQ1 not only targets BRD4 but also BRD2 and BRD3, and as such, previous JQ1-based degraders such as MZ1 have led to the loss of BRD2, BRD3, and BRD4.[23,24] In contrast, NF90 did not degrade BRD2 or BRD3 in MDA-MB-231 cells (Figure S3D,E). We further demonstrated that the BRD4 degradation by NF90 was attenuated by pre-treatment of MDA-MB-231 cells with the proteasome inhibitor bortezomib or the NEDDylation inhibitor MLN4924 (Figure 3E). These latter data indicate that the observed degradation of the BRD4 short isoform is occurring through UBE2D in the complex with a Cullin E3 ligase complex, rather than with another class of E3 ligases (e.g., RING), and suggests that UBE2D is not sufficient to drive degradation of targeted proteins alone.

To confirm that our observed effects were on-target, we showed that the degradation of the BRD4 short isoform was completely attenuated upon knockdown of all four UBE2D1, UBE2D2, UBE2D3, and UBE2D4 enzymes (Figure 3F,G). We also synthesized a nonreactive analog of NF90 with NF457 expecting this degrader to not show UBE2D binding or target degradation. Unexpectedly, we still observed binding of this nonreactive PROTAC to UBE2D2 C85S protein by gel-based ABPP and degradation of the BRD4 short isoform in MDA-MB-231 cells, albeit to a lesser degree than NF90 (Figure S4A–C). These data indicate that EN67 has a significant degree of reversible binding to UBE2D beyond the reactivity introduced by the acrylamide warhead. Because NF90 only degraded one isoform of BRD4, we did not perform quantitative proteomic studies given that we likely did not observe a high degree of total BRD4 loss. The observed selective degradation of only the short isoform of BRD4 is particularly interesting given previous studies that showed tumor suppressive roles of the long isoform of BRD4 and the oncogenic roles of the short BRD4 isoform.[25]

To demonstrate that our EN67 UBE2D recruiter was capable of degrading additional targets beyond BRD4, we next deployed this recruiter to generate androgen receptor (AR) degraders. We linked our EN67 recruiter onto an analog of the AR-targeting ligand from the Arvinas AR PROTAC ARV-110 via C4, C5, and C7 alkyl linkers to generate NF500A, NF500B, and NF500C, respectively (Figures 4A and S5A). We tested these PROTACs alongside the AR-targeting ligand control (NF505) as well as the ARV-110 PROTAC in AR-positive LNCaP prostate cancer cells. While all three PROTACs degraded AR, NF500C with the C7 alkyl linker showed the highest degree of AR degradation (Figures 4B and S5B,C). We further demonstrated that this loss of AR was attenuated by a NEDDylation inhibitor MLN4924 that inhibits Cullin E3 ligases, albeit MLN4924 treatment alone appeared to lower AR levels (Figure 4C). To assess the selectivity of AR degradation, we performed tandem mass tagging (TMT)-based quantitative proteomic profiling of NF500C in LNCaP cells. We showed that AR was the only target degraded by >2-fold with adjusted p-value less than 0.001 (Figure 4D and Table S3). We also generated a nonreactive analogue of NF500C, NF534 and showed that this nonreactive PROTAC still degraded AR to an equivalent degree as NF500C (Figure S6A,B).

https://doi.org/10.1021/acschembio.3c00040
ACS Chem. Biol. XXXX, XXX, XXX−XXX

CONCLUSIONS

In this study, we report the discovery of a covalent recruiter for an E2 conjugating enzyme UBE2D that can be used in heterobifunctional PROTACs to degrade neo-substrates, including BRD4 and AR. We had initially expected that the substrate scope might be broader for an E2 recruiter than an E3 ligase substrate receptor recruiter. However, we observed an even more specific substrate scope with BRD4 where we observed isoform-specific degradation of the short, but not the longer isoform of BRD4. These data are particularly interesting given previous studies demonstrating the opposing tumor suppressive and oncogenic roles of the long versus short isoforms of BRD4, respectively.[25] Our selective short isoform-specific BRD4 degrader may potentially eliminate the oncogenic roles of BRD4 while maintaining its tumor suppressive functions. Currently, however, we do not yet understand the mechanism through which we are achieving selective degradation of only the short isoform of BRD4. We postulate that potentially the long BRD4 isoform may interfere with ternary complex formation with UBE2D.

Attenuation of target degradation by NEDDylation inhibitors indicated that we required the NEDDylated Cullin complex to enable ubiquitination. However, we do not yet know whether recruitment of the E2 potentially bypasses the necessity for an E3 ligase substrate adapter. Formation of the ternary complex with the E2 in the Cullin complex versus the E3 ligase substrate receptor may restrict the geometry of the ternary complex for ubiquitination of the neo-substrate. Future structural elucidation of the Cullin complex with the protein targets may yield insight into the mechanism through which we are bringing together the E2 and the Cullin complex with the neo-substrates to facilitate ubiquitination.

Nonetheless, our study broadens the scope of UPS machinery that can be exploited for PROTACs to now include E2 ubiquitin conjugating enzymes and further highlights the utility of covalent chemoproteomic approaches in rapidly discovering allosteric covalent ligands that can be used as recruiters for induced proximity-based approaches.

METHODS

Chemicals. Screening compounds were purchased from Enamine. Structures and compound names are listed in Table S1. Compounds synthesized in this study are described in Supporting Information.

Gel-Based ABPP. UBE2D2 (C85S) (0.1 μg/25 μL in phosphate-buffered saline (PBS)) was treated with either DMSO vehicle or covalent ligand at 37 °C for 30 min and subsequently treated with 0.1 μM IA-rhodamine (Setareh Biotech) for 1 h at RT in the dark. The reaction was stopped by the addition of 4 × reducing Laemmli SDS sample loading buffer (Alfa Aesar). After boiling at 95 °C for 5 min, the samples were separated on precast 4−20% Criterion TGX gels (Bio-Rad). Probe-labeled proteins were analyzed by in-gel fluorescence using a ChemiDoc MP (Bio-Rad).

Cell Culture. HEK293T cells were obtained from the UC Berkeley Cell Culture Facility and were cultured in Dulbecco's modified Eagle medium (DMEM) containing 10% (v/v) fetal bovine serum (FBS) and maintained at 37 °C with 5% CO_2. MDA-MB-231 cells were obtained from the UC Berkeley Cell Culture Facility and were cultured in Dulbecco's modified Eagle medium (DMEM) containing 10% (v/v) FBS and maintained at 37 °C with 5% CO_2. LNCaP cells were obtained from the American Type Culture Collection (ATCC) and were cultured in RPMI-1640 medium containing 10% (v/v) FBS and maintained at 37 °C with 5% CO_2. Unless otherwise specified, all cell culture materials were purchased from Gibco. It is not known whether HEK293T cells are from male or female origin.

Preparation of Cell Lysates. Cells were washed twice with cold PBS, scraped, and pelleted by centrifugation (700*g*, 5 min, 4 °C). Pellets were resuspended in RIPA buffer (supplemented with protease inhibitor cocktail, ThermoFisher, A32963) for western blot analysis. For all other experiments, cells were resuspended in PBS (supplemented with protease inhibitor cocktail ThermoFisher, A32963) and sonicated. Cells were clarified by centrifugation (12,000*g*, 10 min, 4 °C), and the lysate was transferred to new low-adhesion microcentrifuge tubes. Proteome concentrations were determined using BCA assay, and the lysate was diluted to appropriate working concentrations.

Western Blotting. Proteins were resolved by sodium dodecyl sulfate poly(acrylamide) gel electrophoresis (SDS/PAGE) and transferred to nitrocellulose membranes using the Trans-Blot Turbo transfer system (Bio-Rad). Membranes were blocked with 5% BSA in Tris-buffered saline containing Tween 20 (TBST) solution for 1 h at RT and probed with primary antibody diluted in recommended diluent per manufacturer overnight at 4 °C. After three washes with TBS-T, the membranes were incubated in the dark with IR680- or IR800-conjugated secondary antibodies at 1:10,000 dilution in 5% BSA in TBS-T for 1 h at RT. After three additional washes with TBST, blots were visualized using an Odyssey Li-Cor fluorescent scanner. The membranes were stripped using ReBlot Plus Strong Antibody Stripping Solution (EMD Millipore) when additional primary antibody incubations were performed. Antibodies used in this study were GAPDH (Cell Signaling Technology, 14C10), BRD4 (Abcam, ab128874), BRD2 (Abcam, ab139690), BRD3 (Abcam, ab50818), UBE2D1 (ThermoFisher, CF803633), UBE2D2 (Abcam, ab155088), UBE2D3 (Abcam, ab176568), UBE2D4 (ThermoFisher, TA810786), androgen receptor (Cell Signaling Technology, 5153S), and Anti-DDDDK tag (Abcam, ab205606).

Expression and Purification of UBE2D. Hi-control BL21(DE3) cells were transformed with plasmids expressing UBE2D1, UBE2D1-(C85S), UBE2D1(C85S/C111S), UBE2D2, UBE2D2(C85S), or UBE2D2(C85S/C111S), each containing an N-terminal polyhistidine tag followed by an HRV3C protease cleavage site. Growths were performed with mild shaking at 37 °C using Terrific Broth, with induction of protein expression by treatment with 0.5 mM IPTG once cultures reached an OD_{600} of 1.5−2.0. Cells were then allowed to grow overnight at 19 °C. Cells were collected by centrifugation and then resuspended in lysis buffer (50 mM Tris pH 8.0, 400 mM NaCl, 1 mM TCEP) prior to lysis by three passes through a cell homogenizer at 18,000 psi. Whole cell lysate was then cleared via centrifugation at 45,000*g* for 30 min, prior to loading onto 5 mL of Ni-NTA resin pre-equilibrated with lysis buffer. After loading, the resin was washed with 5 CV each of lysis buffer with increasing concentrations of imidazole (10, 20, 40 mM) followed by elution with lysis buffer + 500 mM imidazole. The polyhistidine tag was then cleaved with treatment with HRV3C protease while dialyzing against 3 L of lysis buffer (0 imidazole) overnight at 4 °C. The protein was then run over 5 mL of Ni-NTA resin (pre-equilibrated with lysis buffer) again, this time collecting the flow-through, which was concentrated and then run over a superdex 75 16/60 column for size exclusion chromatography (flow rate = 1 mL/min). Included fractions containing protein were pooled and concentrated to about 12 mg/mL. Total yield from 1 L of bacteria was approximately 70 mg; this was similar between isoforms and variants. At each step, the correct molecular weight of the protein was confirmed by ESI-LC/MS.

UBE2D2 In Vitro Ubiquitination Assay. UBE2D2 (5.2 μL, 25 μM, Boston Biochem. Inc., E2-622-100) was diluted in TBS (19.6 μL) and incubated with 0.5 μL of DMSO vehicle or EN67 (10 μM final concentration) for 30 min at 37 °C. Subsequently, UBE1 (1.9 μL, 1 μM, Boston Biochem. Inc., E-305-025) was added, followed by MDM2 (1.4 μL, 5 μM, Boston Biochem. Inc., E3-204-050), p53 (17.4 μL, 2 μM, Boston Biochem. Inc., SP454020), FLAG-ubiquitin (1 μL, 10 mg/mL, Boston Biochem. Inc., U12001M), $MgCl_2$ (1 μL, 500 mM), DTT (1 μL, 500 mM), and ATP (1 μL, 100 mM) to achieve a final volume of 50 μL. The mixture was incubated at 37 °C for 4 h with agitation. Then, 20 μL of Laemmli SDS sample loading buffer (Alfa Aesar) was added to quench the reaction and proteins were analyzed by Western Blot. All dilutions were made using 50 mM TBS.

https://doi.org/10.1021/acschembio.3c00040
ACS Chem. Biol. XXXX, XXX, XXX−XXX

Mapping of EN67 Site of Modification on UBE2D2 by LC-MS/MS. UBE2D2 (100 μg, Boston Biochem. Inc., E2-622-100) was diluted in PBS (1 mL) and pre-incubated with EN67 (10 μM final concentration) for 45 min at 37 °C. The protein was precipitated by the addition of 250 μL of TCA (100% w/v) and incubation at −80 °C overnight. The sample was then spun at 20,000*g* for 10 min at 4 °C. The supernatant was carefully removed, and the sample was washed three times with 200 μL of ice-cold 0.01 M HCl/90% acetone solution, with spinning at 20,000 for 5 min at 4 °C between washes. The sample was then resuspended in 30 μL of 8M urea in PBS and 30 μL of ProteaseMax surfactant (20 μg/mL in 100 mM ammonium bicarbonate, Promega, V2071) with vortexing. Ammonium bicarbonate (40 μL, 100 mM) was then added for a final volume of 100 μL. The sample was reduced with 10 μL of TCEP (10 mM final concentration) for 30 min at 60 °C and alkylated with 10 μL of iodoacetamide (12.5 mM final concentration) for 30 min at 37 °C. The sample was then diluted with 120 μL of PBS before 1.2 μL of ProteaseMax surfactant (0.1 mg/mL in 100 mM ammonium bicarbonate, Promega, V2071) and sequencing grade trypsin (10 μL, 0.5 mg/mL in 50 mM ammonium bicarbonate, Promega, V5111) were added for overnight incubation at 37 °C. The next day, the sample was acidified with formic acid (5% final concentration) and fractionated using high pH reversed-phase peptide fractionation kits (ThermoFisher, 84868) according to manufacturer's protocol.

Pulldown of UBE2D2 from HEK293T Cells with an NF363C Probe. HEK293T cells were treated at 70% confluency with DMSO or NF363C (50 μM) for 24 h. Cells were harvested, lysed via sonication, and the resulting lysate normalized to 5 mg/mL per sample. 500 μL of each lysate sample was incubated for 1 h at RT with 10 μL of 10 mM biotin picolyl azide (in DMSO) (Sigma Aldrich 900912), 10 μL of 50 mM TCEP (in H_2O), 30 μL of TBTA ligand (0.9 mg/mL in 1:4 DMSO/*t*BuOH), and 10 μL of 50 mM $CuSO_4$. Proteins were precipitated, washed three times with cold MeOH, resolubilized in 200 μL of 1.2% SDS/PBS (w/v), and heated for 5 min at 90 °C. 10 μL of each sample was removed for Western Blot analysis of the input. To the remaining 190 μL was added 1 mL of PBS and 50 μL of streptavidin agarose beads (ThermoFisher, 20353). Samples were incubated at 4 °C overnight on a rotator. The following day, the samples were warmed to RT and washed with 0.2% SDS and further washed three times with 500 μL of PBS and three times with 500 μL of H_2O to remove nonprobe-labeled proteins. The washed beads were resuspended in 30 μL of Laemmli SDS sample loading buffer (Alfa Aesar), heated to 95 °C for 5 min, and analyzed by Western Blot.

Proteomics Methods. IsoDTB-ABPP and TMT-based quantitative proteomic methods are described in Supporting Information.

Knockdown Studies. RNA interference was performed using siRNA purchased from Dharmacon. HEK293T cells were seeded at 250,000 cells per 6 cm plate and allowed to adhere overnight. Cells were transfected with either 33 nM non-targeting (ON-TARGETplus Non-targeting Control Pool, Dharmacon, D-001810-10-20) or 16.5 nM anti-UBE2D1 (Dharmacon, L-009387-00-0005), anti-UBE2D2 (Dharmacon, L-010383-00-0005), anti-UBE2D3 (Dharmacon, L-008478-00-0005), and anti-UBE2D4 siRNA (Dharmacon, L-009435-00-0005) using 5 μL of Lipofectamine 2000 (ThermoFisher, 11668027). Transfection reagent was added to Opti-MEM (ThermoFisher, 31985070) media and allowed to incubate for 5 min at RT. Meanwhile, siRNA was added to an equal amount of Opti-MEM. Solutions of transfection reagent and siRNA in Opti-MEM were then combined and allowed to incubate for 30 min at RT. These combined solutions were diluted with complete DMEM to provide 2 mL per well, and the media exchanged. Cells were incubated with transfection reagents for 48 h, at which point the media was replaced with media containing DMSO or NF90 (10 μM) and incubated for another 24 h. Cells were then harvested, and protein abundance was analyzed by Western blotting.

■ ASSOCIATED CONTENT

Supporting Information

The Supporting Information is available free of charge at https://pubs.acs.org/doi/10.1021/acschembio.3c00040.

Gel-based ABPP screening data (Table S1); cysteine chemoproteomic profiling data (Table S2); TMT-based quantitative proteomic data (Table S3); characterization of a BRD4 degrader (Figure S1); characterization of an EN67-based BRD4 degrader (Figure S2); further characterization of the BRD4 degrader (Figure S3), characterization of a nonreactive NF90 analog (Figure S4); characterization of an AR degrader (Figure S5); characterization of a nonreactive AR degrader (Figure S6); and supporting methods (PDF)

v2_with structures (XLSX)

Contrast_table_results (XLSX)

Filename-21 (XLSX)

■ AUTHOR INFORMATION

Corresponding Author

Daniel K. Nomura − *Department of Chemistry, University of California, Berkeley, Berkeley, California 94720, United States; Novartis-Berkeley Translational Chemical Biology Institute, Berkeley, California 94720, United States; Innovative Genomics Institute, Berkeley, California 94704, United States; Department of Molecular and Cell Biology, University of California, Berkeley, Berkeley, California 94720, United States;* orcid.org/0000-0003-1614-8360; Email: dnomura@berkeley.edu

Authors

Nafsika Forte − *Department of Chemistry, University of California, Berkeley, Berkeley, California 94720, United States; Novartis-Berkeley Translational Chemical Biology Institute, Berkeley, California 94720, United States; Innovative Genomics Institute, Berkeley, California 94704, United States*

Dustin Dovala − *Novartis-Berkeley Translational Chemical Biology Institute, Berkeley, California 94720, United States; Novartis Institutes for BioMedical Research, Emeryville, California 94608, United States*

Matthew J. Hesse − *Novartis-Berkeley Translational Chemical Biology Institute, Berkeley, California 94720, United States; Novartis Institutes for BioMedical Research, Emeryville, California 94608, United States*

Jeffrey M. McKenna − *Novartis-Berkeley Translational Chemical Biology Institute, Berkeley, California 94720, United States; Novartis Institutes for BioMedical Research, Cambridge, Massachusetts 02139, United States*

John A. Tallarico − *Novartis-Berkeley Translational Chemical Biology Institute, Berkeley, California 94720, United States; Novartis Institutes for BioMedical Research, Cambridge, Massachusetts 02139, United States*

Markus Schirle − *Novartis-Berkeley Translational Chemical Biology Institute, Berkeley, California 94720, United States; Novartis Institutes for BioMedical Research, Cambridge, Massachusetts 02139, United States;* orcid.org/0000-0003-4933-2623

Complete contact information is available at: https://pubs.acs.org/10.1021/acschembio.3c00040

Author Contributions

N.F. and D.K.N. conceived of the project idea, designed experiments, performed experiments, analyzed and interpreted the data, and wrote the paper. N.F., D.K.N., and D.D. performed experiments, analyzed and interpreted data, and provided intellectual contributions. D.D., M.J.H., J.A.T., J.M.M., and

https://doi.org/10.1021/acschembio.3c00040
ACS Chem. Biol. XXXX, XXX, XXX−XXX

M.S. provided intellectual contributions to the project and overall design of the project.

Notes

The authors declare the following competing financial interest(s): JAT, JMK, DD, MJH, MS are employees of Novartis Institutes for BioMedical Research. This study was funded by the Novartis Institutes for BioMedical Research and the Novartis-Berkeley Translational Chemical Biology Institute. DKN is a co-founder, shareholder, and scientific advisory board member for Frontier Medicines and Vicinitas Therapeutics. DKN is a member of the board of directors for Vicinitas Therapeutics. DKN is also on the scientific advisory board of The Mark Foundation for Cancer Research, MD Anderson Cancer Center, Photys Therapeutics, Apertor Pharmaceuticals, Oerth Bio, and Chordia Therapeutics. DKN is also an Investment Advisory Board member for Droia Ventures and a16z.

J.A.T., J.M.K., D.D., M.J.H., and M.S. are employees of Novartis Institutes for BioMedical Research. This study was funded by the Novartis Institutes for BioMedical Research and the Novartis-Berkeley Translational Chemical Biology Institute. D.K.N. is a co-founder, shareholder, and scientific advisory board member for Frontier Medicines and Vicinitas Therapeutics. D.K.N. is a member of the board of directors for Vicinitas Therapeutics. D.K.N. is also on the scientific advisory board of The Mark Foundation for Cancer Research, MD Anderson Cancer Center, Photys Therapeutics, Apertor Pharmaceuticals, Oerth Bio, and Chordia Therapeutics. D.K.N. is also an Investment Advisory Board member for Droia Ventures and a16z.

■ ACKNOWLEDGMENTS

The authors thank the members of the Nomura Research Group and Novartis Institutes for BioMedical Research for critical reading of the manuscript. This work was supported by Novartis Institutes for BioMedical Research and the Novartis-Berkeley Translational Chemical Biology Institute (NB-TCBI) for all listed authors. This work was also supported by the Nomura Research Group and the Mark Foundation for Cancer Research ASPIRE Award for D.K.N. and N.F. This work was also supported by grants from the National Institutes of Health (R01CA240981 and R35CA263814 for D.K.N.) and the National Science Foundation Molecular Foundations for Biotechnology Award (2127788). The authors also thank H. Celik, A. Lund, and UC Berkeley's NMR facility in the College of Chemistry (CoC-NMR) for spectroscopic assistance. Instruments in the College of Chemistry NMR facility are supported in part by NIH S10OD024998.

■ REFERENCES

(1) Burslem, G. M.; Crews, C. M. Proteolysis-Targeting Chimeras as Therapeutics and Tools for Biological Discovery. *Cell* **2020**, *181*, 102−114.

(2) Schreiber, S. L. The Rise of Molecular Glues. *Cell* **2021**, *184*, 3−9.

(3) Belcher, B. P.; Ward, C. C.; Nomura, D. K. Ligandability of E3 Ligases for Targeted Protein Degradation Applications. *Biochemistry* **2023**, *62*, 588−600.

(4) Backus, K. M.; Correia, B. E.; Lum, K. M.; et al. Proteome-wide covalent ligand discovery in native biological systems. *Nature* **2016**, *534*, 570−574.

(5) Zhang, X.; Crowley, V. M.; Wucherpfennig, T. G.; Dix, M. M.; Cravatt, B. F. Electrophilic PROTACs that degrade nuclear proteins by engaging DCAF16. *Nat. Chem. Biol.* **2019**, *15*, 737−746.

(6) Zhang, X.; Luukkonen, L. M.; Eissler, C. L.; et al. DCAF11 Supports Targeted Protein Degradation by Electrophilic Proteolysis-Targeting Chimeras. *J. Am. Chem. Soc.* **2021**, *143*, 5141−5149.

(7) Tao, Y.; Remillard, D.; Vinogradova, E. V.; et al. Targeted Protein Degradation by Electrophilic PROTACs that Stereoselectively and Site-Specifically Engage DCAF1. *J. Am. Chem. Soc.* **2022**, *144*, 18688−18699.

(8) Spradlin, J. N.; Hu, X.; Ward, C. C.; et al. Harnessing the anti-cancer natural product nimbolide for targeted protein degradation. *Nat. Chem. Biol.* **2019**, *15*, 747−755.

(9) Luo, M.; Spradlin, J. N.; Boike, L.; et al. Chemoproteomics-enabled discovery of covalent RNF114-based degraders that mimic natural product function. *Cell Chem. Biol.* **2021**, *28*, 559−566.e15.

(10) Ward, C. C.; Kleinman, J. I.; Brittain, S. M.; et al. Covalent Ligand Screening Uncovers a RNF4 E3 Ligase Recruiter for Targeted Protein Degradation Applications. *ACS Chem. Biol.* **2019**, *14*, 2430−2440.

(11) Henning, N. J.; Manford, A. G.; Spradlin, J. N.; et al. Discovery of a Covalent FEM1B Recruiter for Targeted Protein Degradation Applications. *J. Am. Chem. Soc.* **2022**, *144*, 701−708.

(12) Słabicki, M.; Kozicka, Z.; Petzold, G.; et al. The CDK inhibitor CR8 acts as a molecular glue degrader that depletes cyclin K. *Nature* **2020**, *585*, 293−297.

(13) Lv, L.; Chen, P.; Cao, L.; et al. Discovery of a molecular glue promoting CDK12-DDB1 interaction to trigger cyclin K degradation. *eLife* **2020**, *9*, No. e59994.

(14) King, E. A.; Cho, Y.; Hsu, N. S.; Dovala, D.; McKenna, J. M.; Tallarico, J. A.; Schirle, M.; Nomura, D. K. Chemoproteomics-Enabled Discovery of a Covalent Molecular Glue Degrader Targeting NF-κB. *Cell Chemical Biology* **2023**, DOI: 10.1016/j.chembiol.2023.02.008.

(15) Ottis, P.; Palladino, C.; Thienger, P.; et al. Cellular Resistance Mechanisms to Targeted Protein Degradation Converge Toward Impairment of the Engaged Ubiquitin Transfer Pathway. *ACS Chem. Biol.* **2019**, *14*, 2215−2223.

(16) Zhang, L.; Riley-Gillis, B.; Vijay, P.; Shen, Y. Acquired Resistance to BET-PROTACs (Proteolysis-Targeting Chimeras) Caused by Genomic Alterations in Core Components of E3 Ligase Complexes. *Mol. Cancer Ther.* **2019**, *18*, 1302−1311.

(17) Stewart, M. D.; Ritterhoff, T.; Klevit, R. E.; Brzovic, P. S. E2 enzymes: more than just middle men. *Cell Res.* **2016**, *26*, 423−440.

(18) Baek, K.; Krist, D. T.; Prabu, J. R.; et al. NEDD8 nucleates a multivalent cullin−RING−UBE2D ubiquitin ligation assembly. *Nature* **2020**, *578*, 461−466.

(19) Lei, L.; Bandola-Simon, J.; Roche, P. A. Ubiquitin-conjugating enzyme E2 D1 (Ube2D1) mediates lysine-independent ubiquitination of the E3 ubiquitin ligase March-I. *J. Biol. Chem.* **2018**, *293*, 3904−3912.

(20) Weerapana, E.; Wang, C.; Simon, G. M.; et al. Quantitative reactivity profiling predicts functional cysteines in proteomes. *Nature* **2010**, *468*, 790−795.

(21) Zanon, P. R. A.; Lewald, L.; Hacker, S. M. Isotopically Labeled Desthiobiotin Azide (isoDTB) Tags Enable Global Profiling of the Bacterial Cysteinome. *Angew. Chem.* **2020**, *132*, 2851−2858.

(22) Henning, N. J.; Boike, L.; Spradlin, J. N.; et al. Deubiquitinase-targeting chimeras for targeted protein stabilization. *Nat. Chem. Biol.* **2022**, *18*, 412−421.

(23) Filippakopoulos, P.; Qi, J.; Picaud, S.; et al. Selective inhibition of BET bromodomains. *Nature* **2010**, *468*, 1067−1073.

(24) Zengerle, M.; Chan, K.-H.; Ciulli, A. Selective Small Molecule Induced Degradation of the BET Bromodomain Protein BRD4. *ACS Chem. Biol.* **2015**, *10*, 1770−1777.

(25) Wu, S.-Y.; Lee, C. F.; Lai, H. T.; et al. Opposing Functions of BRD4 Isoforms in Breast Cancer. *Mol. Cell* **2020**, *78*, 1114−1132.

https://doi.org/10.1021/acschembio.3c00040
ACS Chem. Biol. XXXX, XXX, XXX−XXX